
Figures and figure supplements

Amotl2a interacts with the Hippo effector Yap1 and the Wnt/ β -catenin effector Lef1 to control tissue size in zebrafish

Sobhika Agarwala, et al.

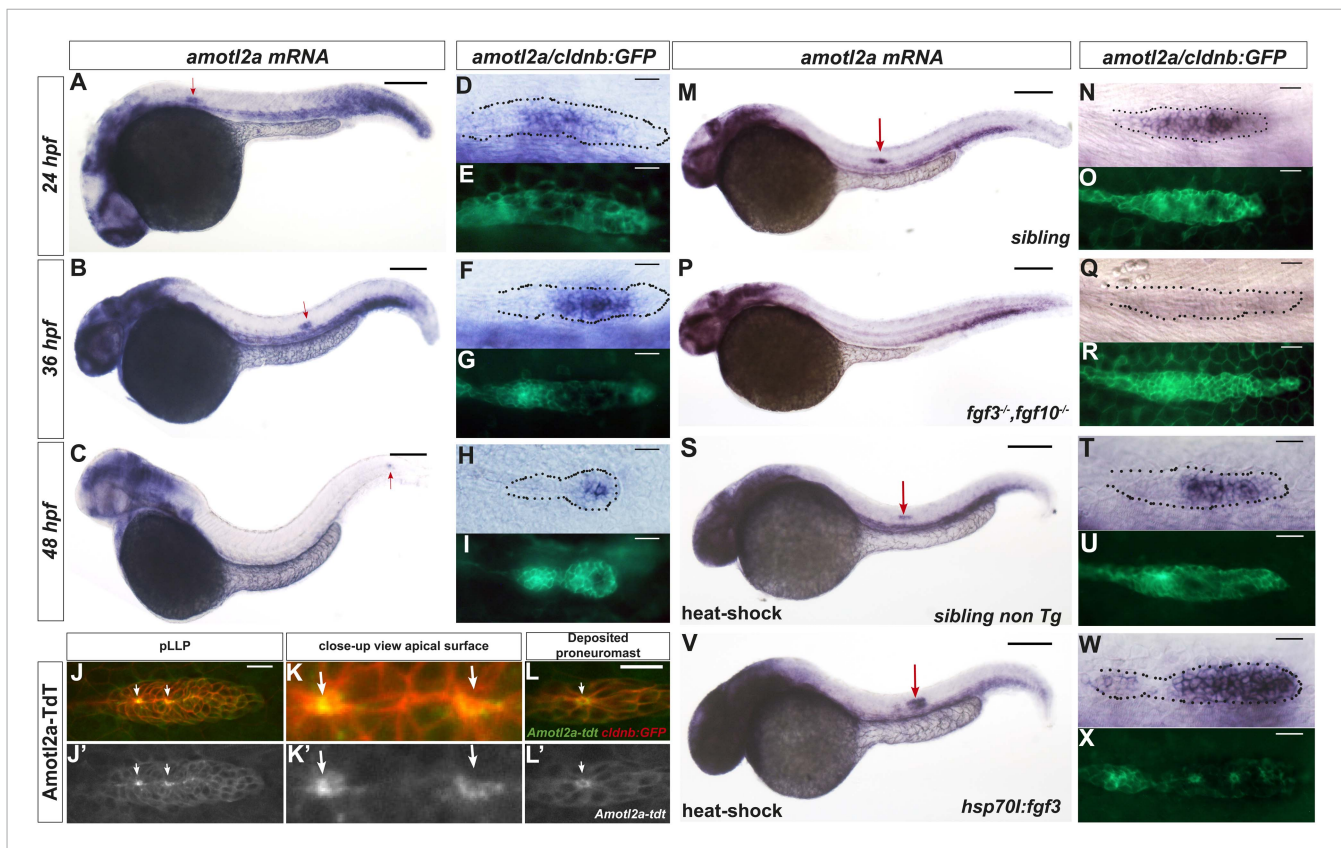


Figure 1. *amotl2a* is expressed in the pLLP and localizes at the cell apical side. (A–I) *cldnb:gfp* embryos stained with an *amotl2a* antisense RNA probe and an anti-GFP antibody (E, G, I) at the indicated stages. Red arrows indicate the posterior lateral line primordium (pLLP). (D–I) Close-up views of the pLLP. (J–L') Maximum intensity projection (MIP) of Z-stacks of the pLLP (J–J') and a recently deposited neuromast (L–L') in *cldnb:gfp* embryos injected with *amotl2a-TdT* mRNA. (K–K') Close-up views of (J–J'). White arrows indicate rosette centers. Colors have been inverted. (M–X) 30 hpf *cldnb:gfp* embryos stained with an *amotl2a* in situ hybridization (ISH) probe and an anti-GFP antibody (O, R, U, X) in the indicated genetic background. The right column shows the primordium at higher magnification. In all figures, scale bars correspond to 200 μ m for whole-embryo images and 20 μ m in close up views of the pLLP. In all figures, n is the total number of embryos/primordia analysed and N is the number of biological replicates (Figure 1—figure supplement 1, Figure 1—source data 1).

DOI: [10.7554/eLife.08201.003](https://doi.org/10.7554/eLife.08201.003)

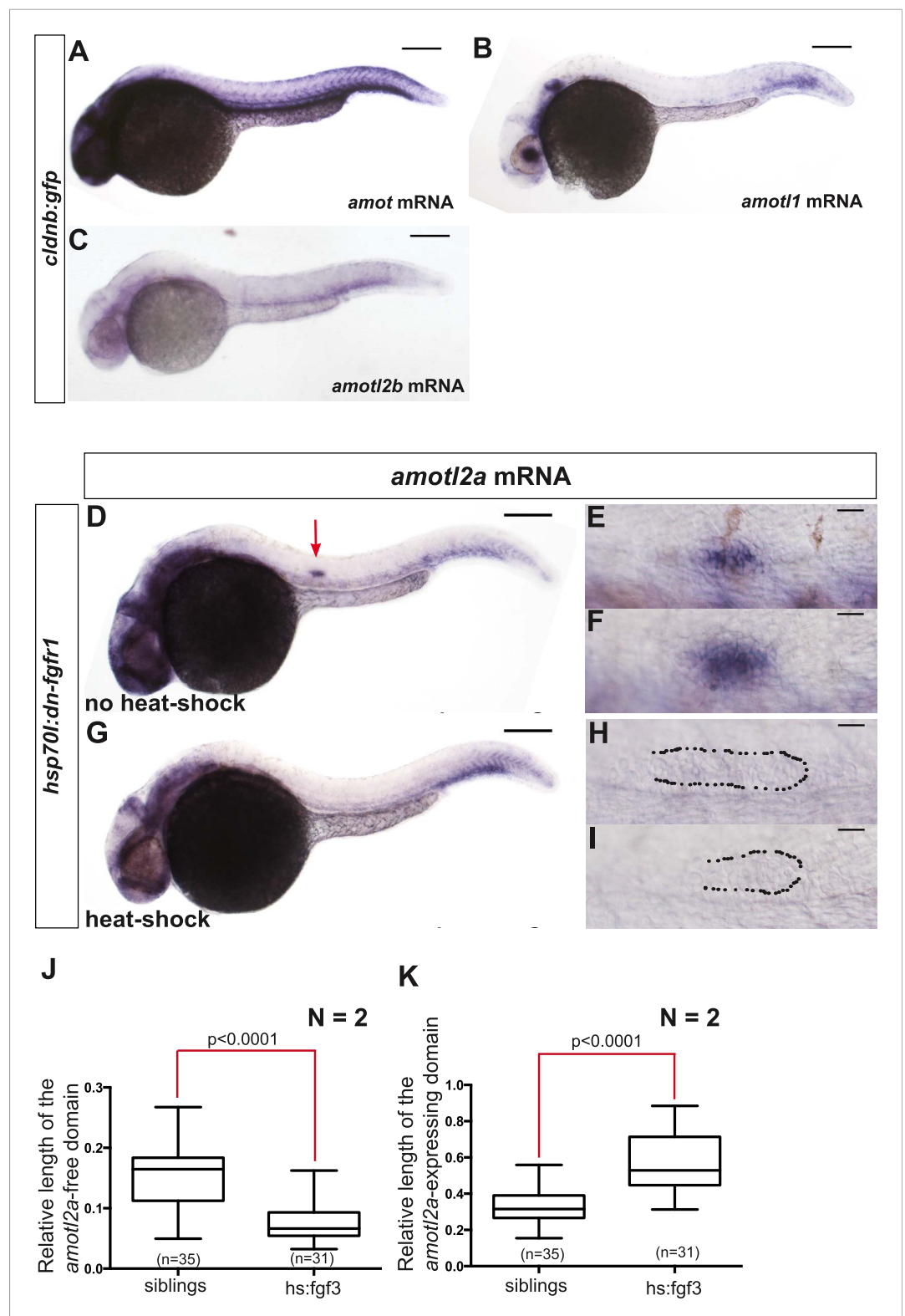


Figure 1—figure supplement 1. Only *amotl2a* is expressed in the pLLP and its expression is controlled by FGF signaling. (A–C) ISH staining with probes against *amot* (A), *amotl1* (B), and *amotl2b* (C) in *cldnb:gfp* embryos. (D–I) ISH staining with an *amotl2a* probe in *Tg(hsp70l:dnfgfr1EGFP)^{pd}* embryos non-heat-shocked (D–F) or heat-shocked (G–I). The red arrow points to the pLLP. The dotted lines indicate the pLLP contour. (J, K) Boxplots showing the

Figure 1—figure supplement 1. continued on next page

Figure 1—figure supplement 1. Continued

comparison of the relative length of the *amotl2a*-free domain (J) and of the *amotl2a*-expressing domain (K) between the indicated groups (**Figure 1—source data 1**).

DOI: [10.7554/eLife.08201.005](https://doi.org/10.7554/eLife.08201.005)

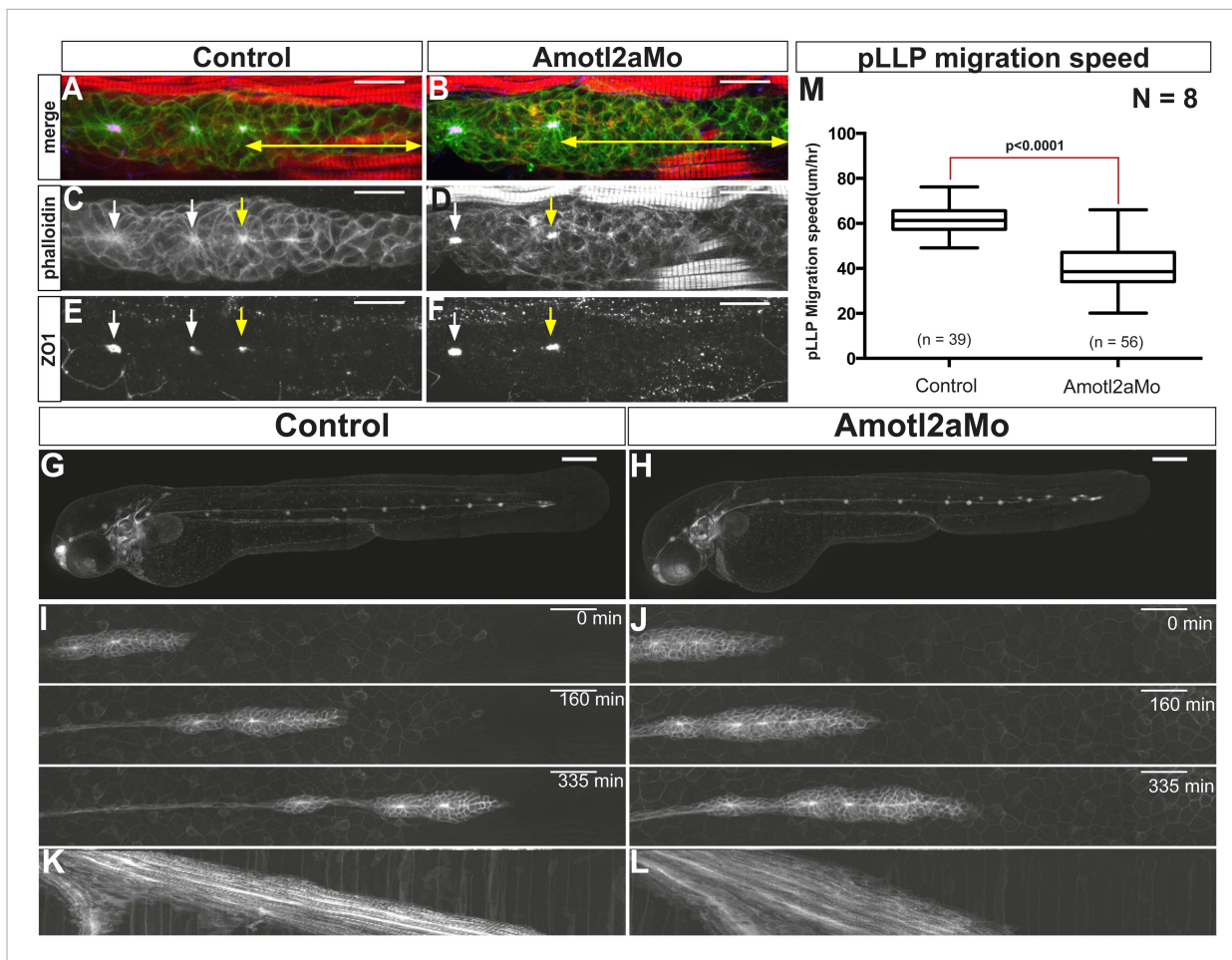


Figure 2. *Amotl2a* is not essential for proneuromast assembly but for proper migration. (A–F) MIP of Z-stacks of pLLP stained with ZO-1 (blue) and GFP (green) antibodies and phalloidin (red) in control (A, C, E) and *amotl2a* morphant (B, D, F) *cldnb:gfp* embryos at 30 hpf. (G, H) MIP of overview images of control (G) and *amotl2a* morphant (H) embryos after completion of migration. (I, J) Snapshots of time-lapse movies at the indicated timepoints showing a delay in migration in *amotl2a* morphants (J) as compared to controls (I). (K, L) Corresponding kymographs used to measure the migration speed. (M) Boxplot comparing the migration speeds (Figure 2—source data 1, Figure 2—figure supplements 1, 2).

DOI: [10.7554/eLife.08201.006](https://doi.org/10.7554/eLife.08201.006)

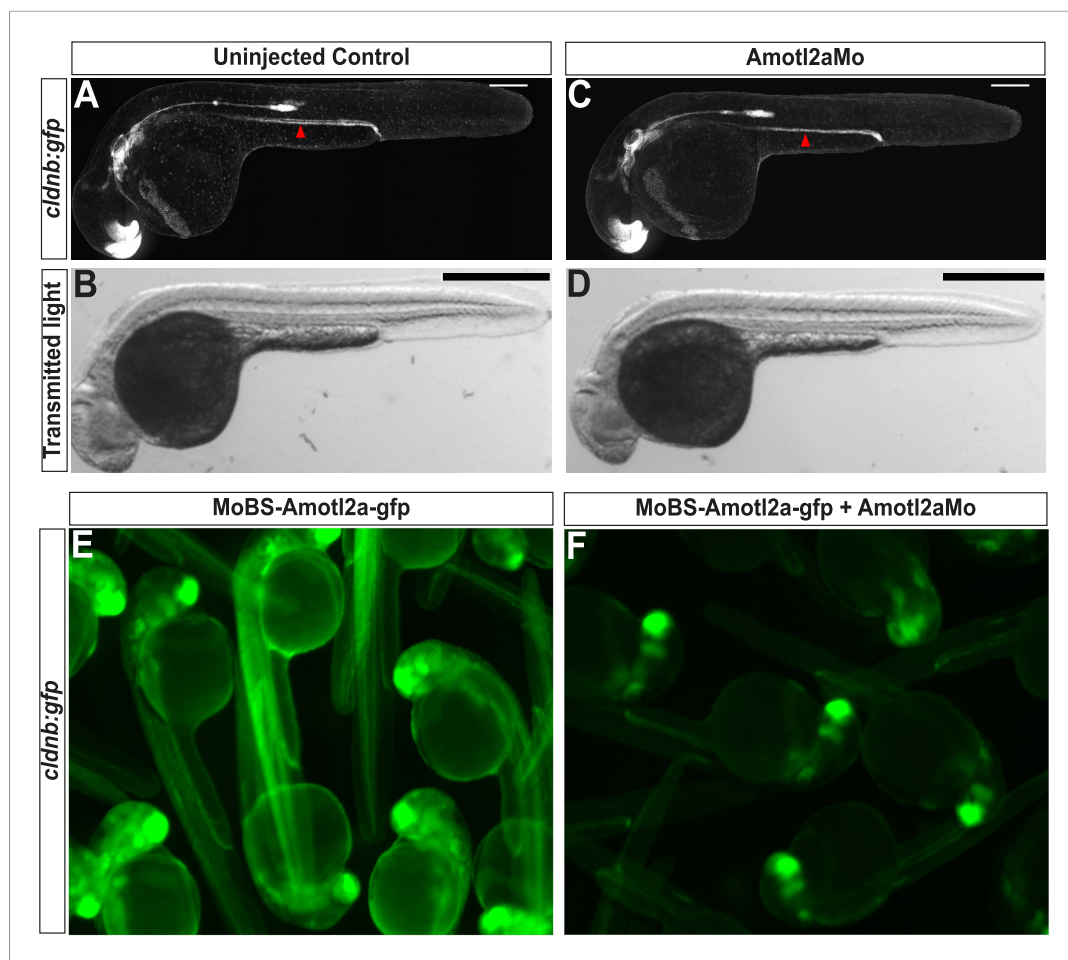


Figure 2—figure supplement 1. Amotl2aMo efficiency. (A–D) Overview pictures of 30 hpf *cldnb:gfp* embryos uninjected (A, B) or injected with Amotl2aMo (C, D), imaged either with fluorescent (A–C) or transmitted light (B–D). (E, F) *cldnb:gfp* embryos injected with RNA encoding the Mo-binding region of Amotl2a fused to GFP (MoBS-*amotl2a-gfp*) either alone (E) or with Amotl2aMo (F). The bright green fluorescence in F comes from the expression of the *cldnb:gfp* transgene in the brain and eyes. The red arrowheads in A and C indicate the level of migration at which embryos were fixed for cell counting quantification (see 'Materials and methods').

DOI: [10.7554/eLife.08201.008](https://doi.org/10.7554/eLife.08201.008)

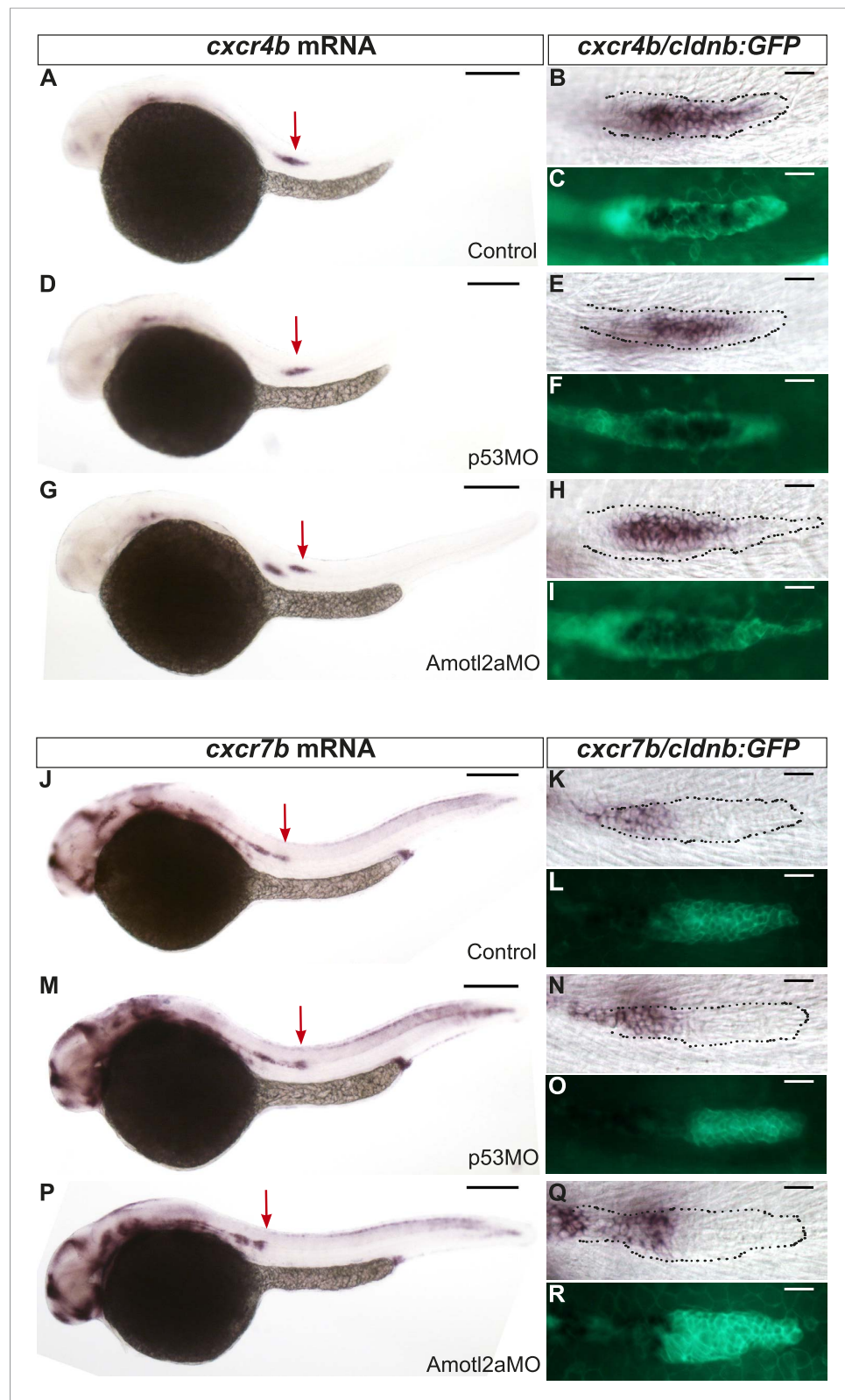


Figure 2—figure supplement 2. *cxcr4b* and *cxcr7b* expression are not affected in *amotl2a* morphants. Uninjected (A–C and J–L), p53Mo-injected (D–F and M–O), or Amotl2aMo-injected (G–I and P–R) *cldnb:gfp* embryos stained with a *cxcr4b* (A–I) or a *cxcr7b* (J–R) ISH probe and an anti-GFP antibody (C, F, I, L, O, R). Red arrows point to the pLLP.

DOI: [10.7554/eLife.08201.009](https://doi.org/10.7554/eLife.08201.009)

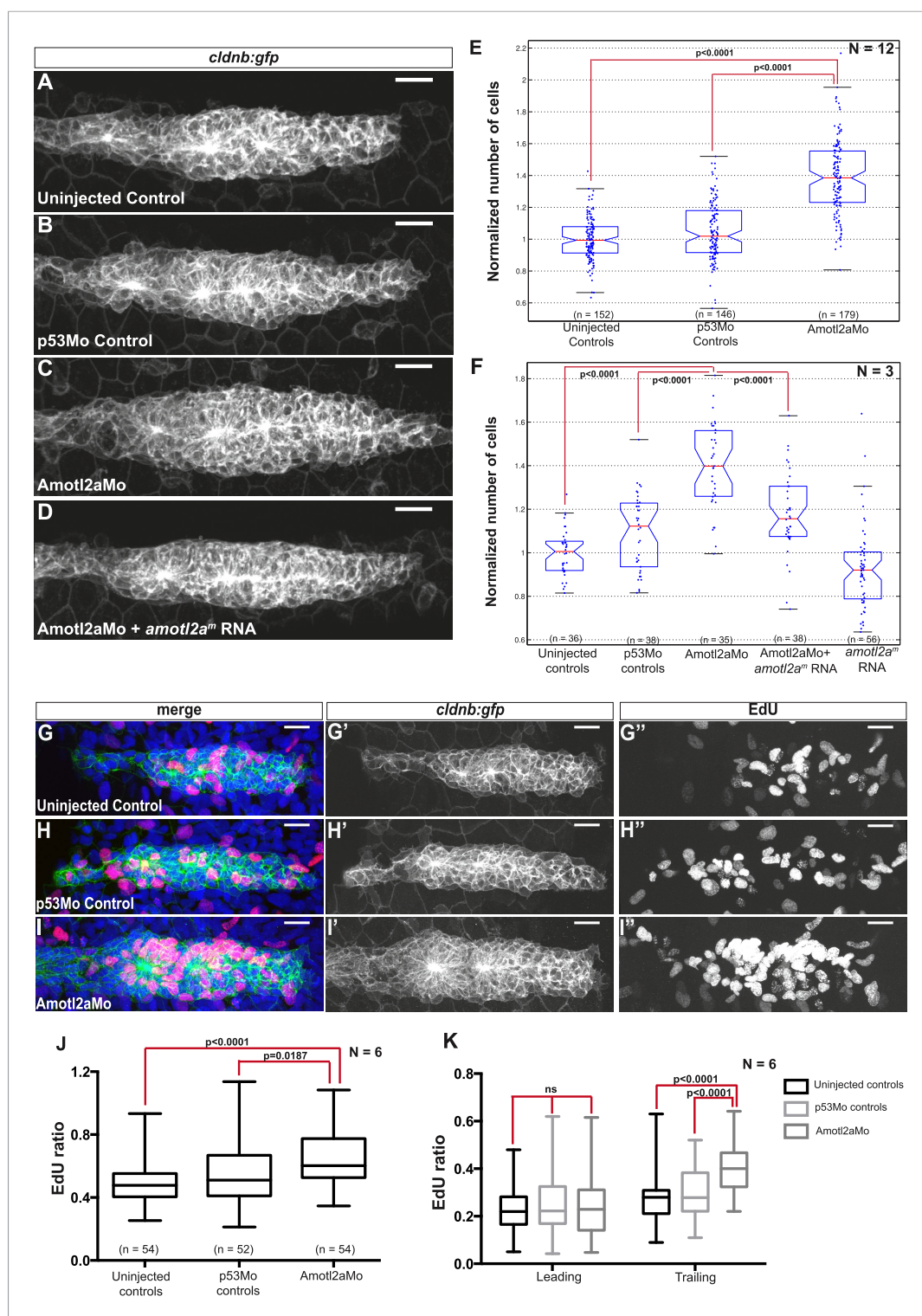


Figure 3. Amotl2a is required to limit proliferation in the pLLP. (A–D) MIP of Z-stacks of pLLP in *cldnb:gfp* embryos injected as indicated. (E, F) Boxplots showing the number of cells in the primordia of indicated groups, normalized to the control group. (G–I') MIP of Z-stacks of pLLP in *cldnb:gfp* embryos stained with EdU and DAPI showing the green (membranes, middle), red (EdU, right), and merge (left) channels. (J, K) Boxplot showing the comparison of the EdU index in the indicated experimental conditions in whole primordia (J) or separately in the leading and trailing region (K) (Figure 3—source data 1–3, Figure 3—figure supplements 1, 2, Figure 3—source data 4).

DOI: 10.7554/eLife.08201.010

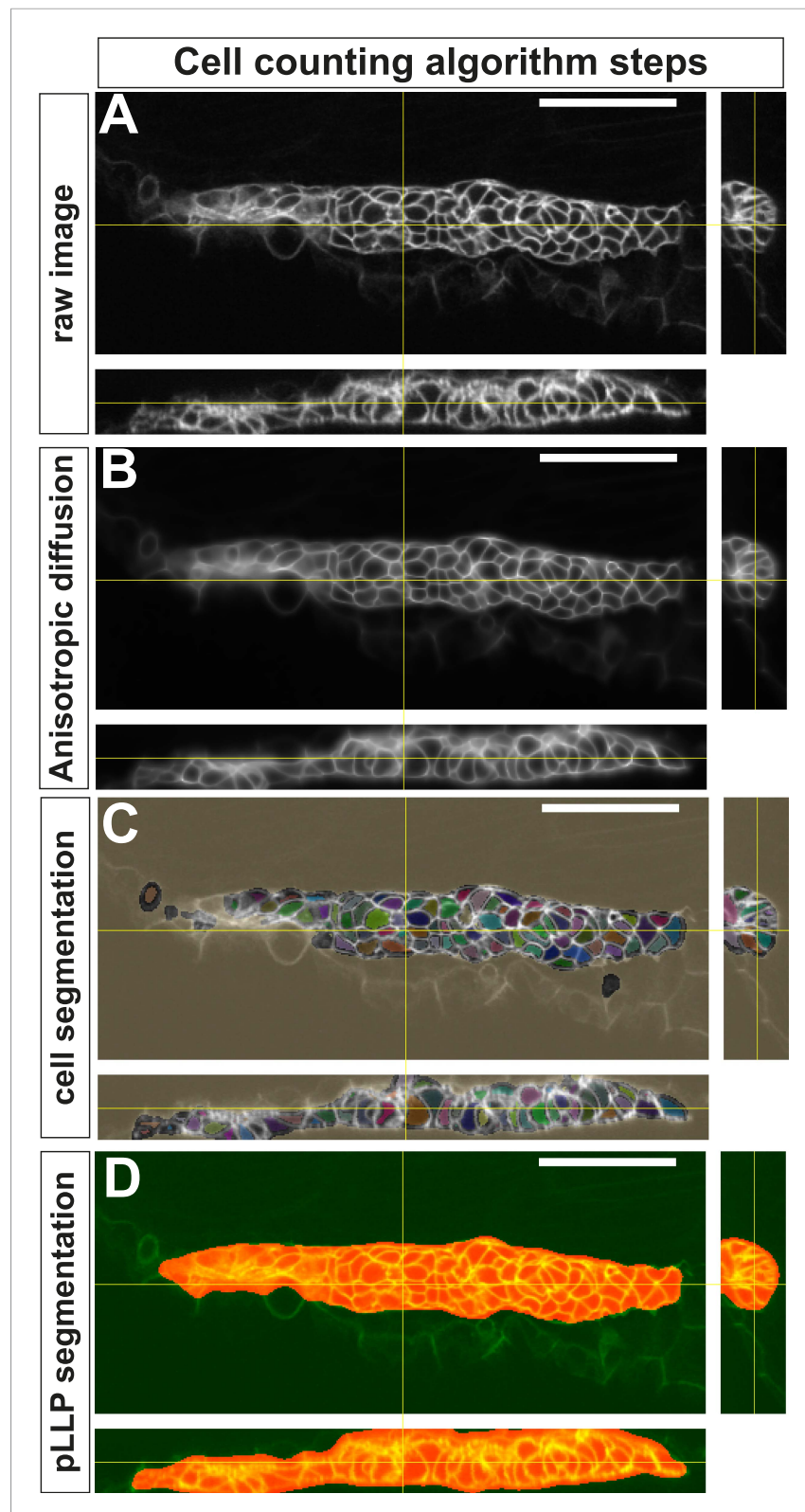


Figure 3—figure supplement 1. Successive steps of the automated ‘cell-counting’ algorithm. (A) Raw image of pLLP in a *cldnb:gfp* embryo. (B) Enhanced, filtered image using anisotropic diffusion. (C) Segmentation of individual cells. (D) Segmentation mask of the pLLP.

DOI: [10.7554/eLife.08201.015](https://doi.org/10.7554/eLife.08201.015)

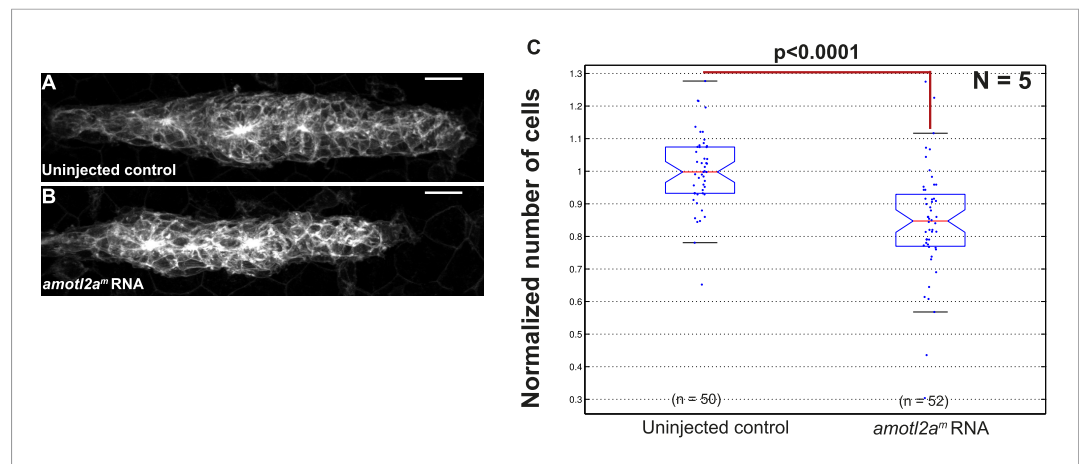


Figure 3—figure supplement 2. Overexpression of *amotl2a* leads to reduced cell number in the pLLP. (A, B) MIP of Z-stacks of pLLP in *cldnb:gfp* embryos injected as indicated. (C) Corresponding boxplot comparing the number of cells in the indicated experimental conditions. (Figure 3—source data 4).

DOI: [10.7554/eLife.08201.016](https://doi.org/10.7554/eLife.08201.016)

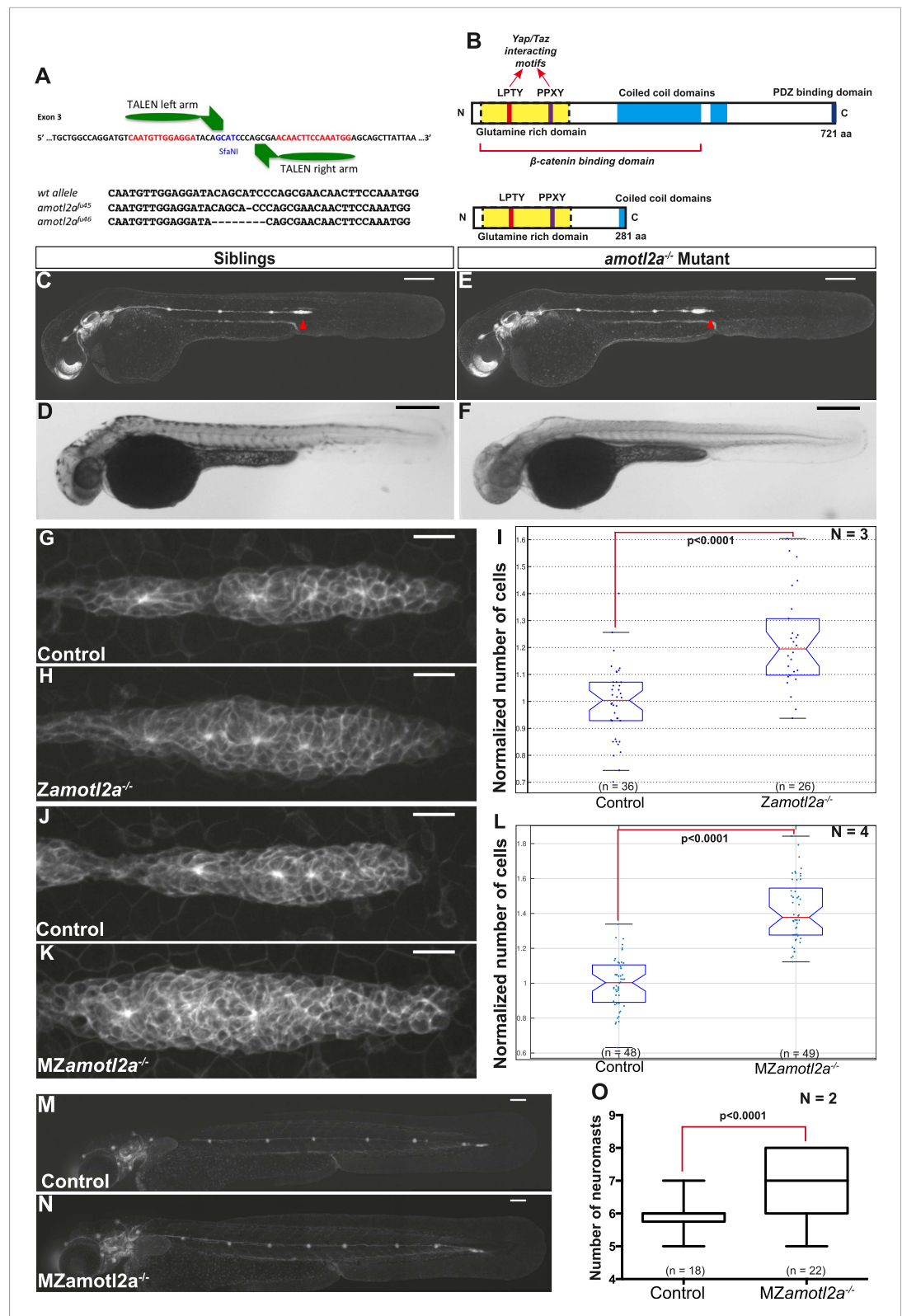


Figure 4. *amotl2a* mutants phenocopy the morphant phenotype. **(A)** Scheme showing the transcription activator-like effector nuclease (TALEN) target site in the *amotl2a* locus with the left and right TALEN-binding sites in red separated by the spacer including the restriction site used for screening (blue) (top). Alignment of the two conserved *amotl2a* mutant alleles with the corresponding wild-type sequence showing the deleted nucleotides (bottom). Figure 4. continued on next page

Figure 4. Continued

(B) Scheme comparing the functional domains present in the wild-type Amotl2a protein (721aa long) and the putative truncated proteins (272aa +17 or +9 missense aa for allele *fu45* and *fu46*, respectively). (C–F) 36 hpf *clnbn:gfp* wild-type sibling (C, D) or *amotl2a^{-/-}* mutant embryo (E, F) imaged with fluorescent (C, E) or transmitted light (D, F). (G, H, J, K) MIP of Z-stacks of pLLP in *clnbn:gfp* embryos with the indicated genetic background. (I, L) Boxplots comparing the cell numbers between the indicated genetic backgrounds. (M, N) MZamotl2a^{-/-} mutant embryo (N) showing an extra deposited neuromast as compared to a wild-type sibling embryo (M). (O) Boxplot showing the corresponding quantification (Figure 4—source data 1, 2; Figure 4—figure supplements 1, 2, Figure 4—source data 3, 4).

DOI: 10.7554/eLife.08201.017

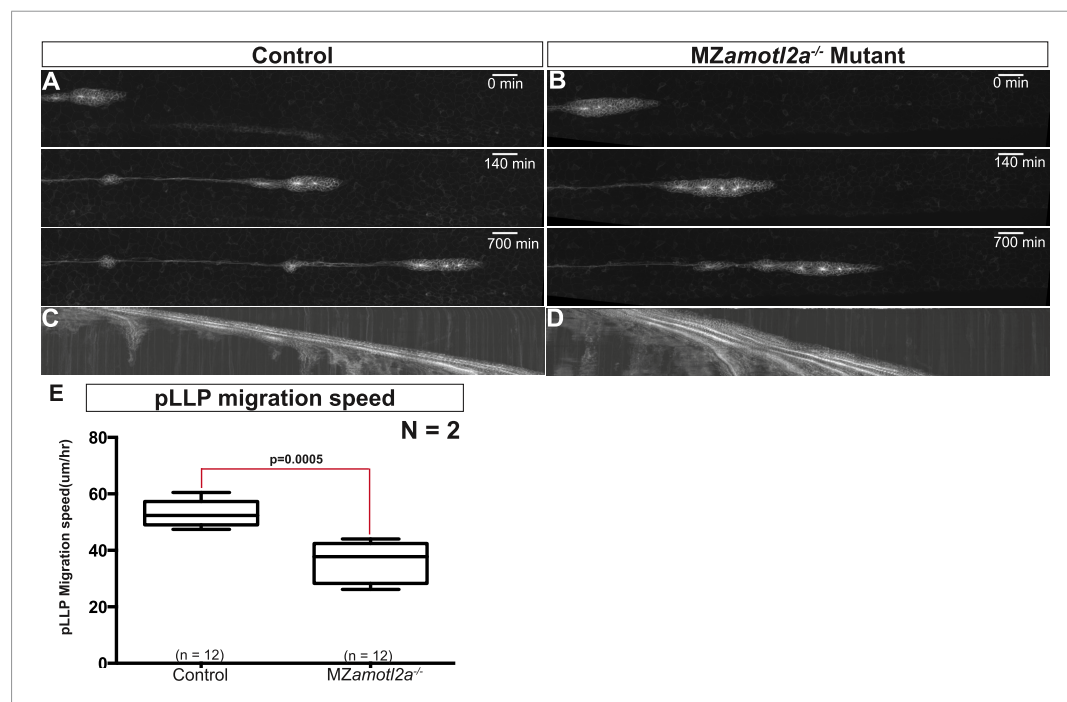


Figure 4—figure supplement 1. MZamotl2a^{-/-} mutants exhibit reduced pLLP migration speed. (A, B) Snapshots of time-lapse movies at the indicated timepoint showing a delay in migration speed in MZamotl2a^{-/-} mutants (B) as compared to siblings (A). (C, D) Corresponding kymographs. (E) Boxplot comparing the migration speeds in control vs MZamotl2a^{-/-} mutant pLLP (Figure 4—source data 3).

DOI: 10.7554/eLife.08201.022

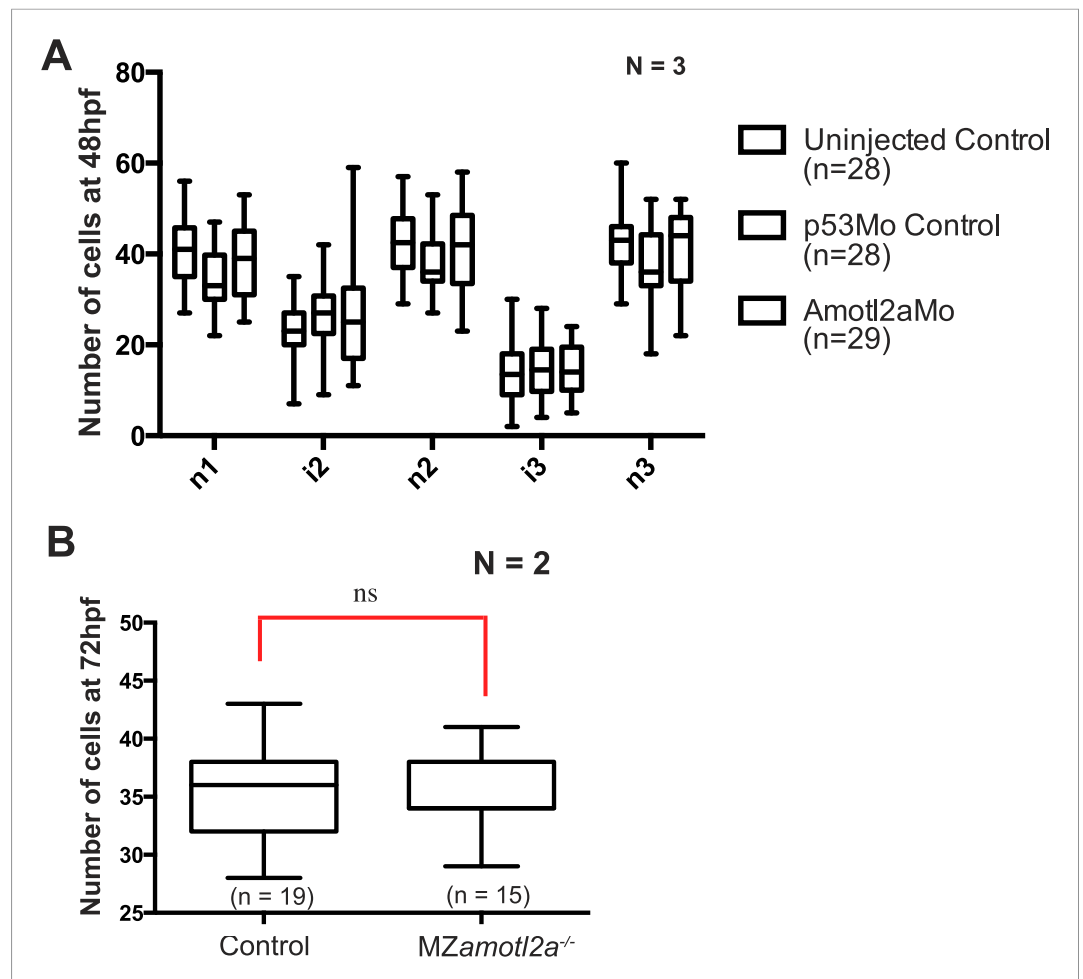


Figure 4—figure supplement 2. Deposited neuromasts or interneuromast chains do not contain more cells in *amotl2a* morphants or mutants. **(A)** Boxplots showing cell number quantifications in the first 3 neuromasts (n1 to n3) and interneuromast regions (i1 and i2) at 48 hpf in the indicated experimental conditions. **(B)** Boxplot showing cell number quantification in one neuromast close to the end of yolk extension (n3 or n4) at 72 hpf in the indicated experimental conditions (**Figure 4—source data 4**).

DOI: [10.7554/eLife.08201.023](https://doi.org/10.7554/eLife.08201.023)

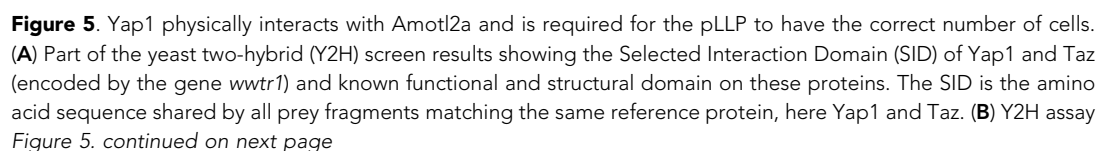


Figure 5. Continued

with Histidine (left panel, growth control) and without Histidine (right panel, protein interaction assay) showing the interactions between zebrafish Amotl2a and Yap1 or Taz (red), but not with the corresponding proteins mutated in the known interaction motifs: LPTY/PPEY for Amotl2a (green) and WW domain for Yap1 and Taz (pink). (C, D) MIP of Z-stacks of pLLP in *cldnb:gfp* embryos injected as indicated. (E) Boxplot comparing the number of cells in the pLLP in Yap1Mo-injected embryos and controls. (F) Scheme showing the TALEN target site in the *yap1* locus with the left and right TALEN-binding sites in red separated by the spacer including the restriction site used for screening (blue) (top). Alignment of the two *yap1* mutant alleles with the corresponding wild-type sequence showing the deleted nucleotides (bottom). (G) Scheme comparing the functional domains present in the wild-type Yap1 (442aa long) and the putative truncated proteins (76aa +25 or +45 missense aa before for allele *fu47* and *fu48*, respectively). (H, I) Overview pictures of 36 hpf *cldnb:gfp* control and *Zyap1^{-/-}* embryos. (J–M) MIP of Z-stacks of pLLP in *cldnb:gfp* embryos with the indicated genotype. (N–P) Boxplot showing cell counts in the pLLP in embryos of the corresponding genotypes (Figure 5—source data 1, 2; Figure 5—figure supplement 1; Figure 5—source data 3, 4).

DOI: [10.7554/eLife.08201.024](https://doi.org/10.7554/eLife.08201.024)

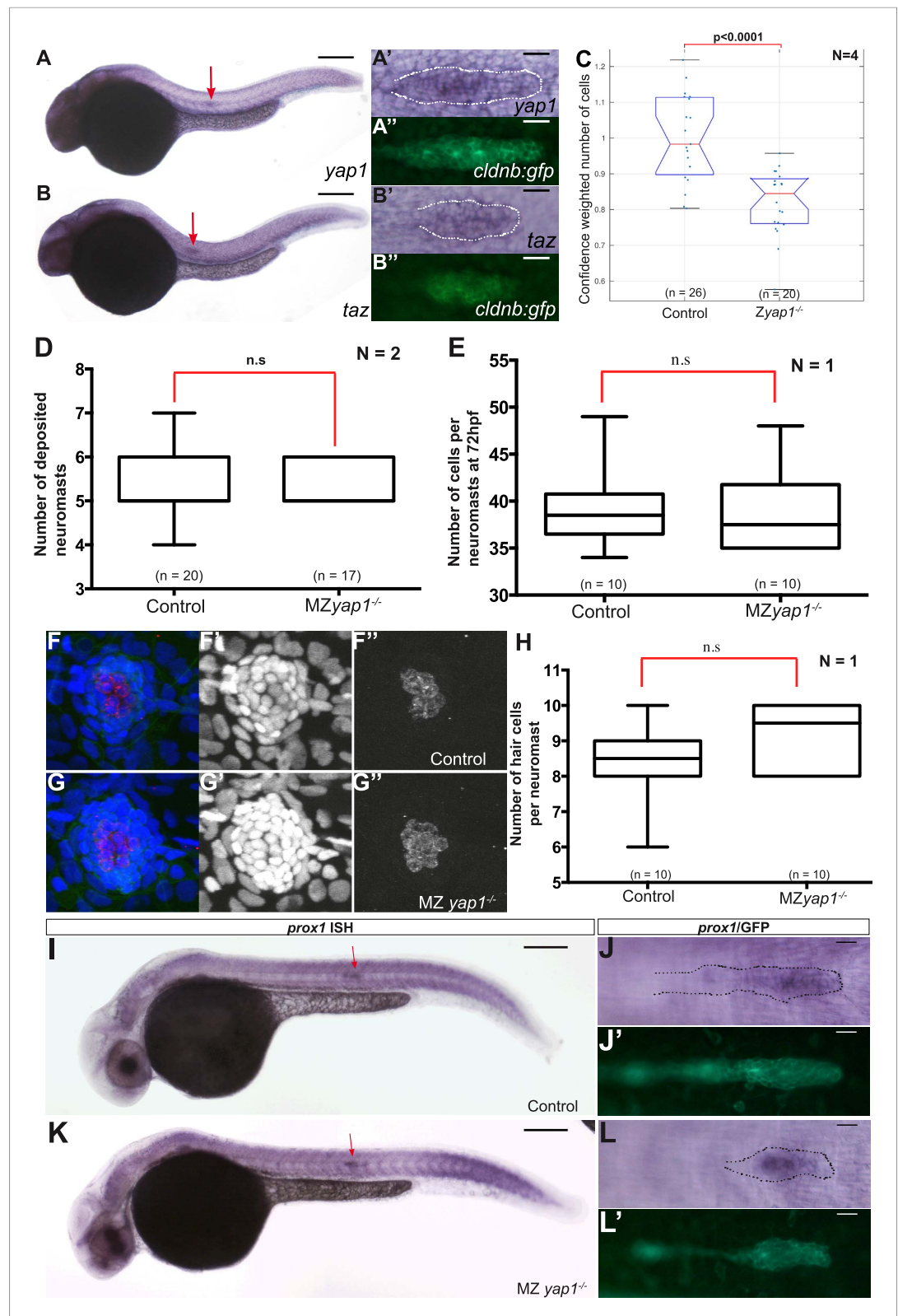


Figure 5—figure supplement 1. *yap1* and *taz* are ubiquitously expressed at 30 hpf. *Zyp1*^{-/-} mutant embryos have fewer cells compared to sibling controls. (A–B'') 30 hpf *cldnb:gfp* embryos stained with a *yap1* (A–A'') or a *taz* (B–B'') ISH probe and an anti-GFP antibody (A', B'). (C–E, H) Boxplot showing pLLP cell counts (C), number of deposited neuromasts (D), number of cells per neuromast at 72 hpf (E), and number of hair cells per neuromast (H) for Control and *MZyap1*^{-/-} embryos. (F–G'') Confocal images of *prox1* ISH and anti-GFP antibody staining in Control and *MZyap1*^{-/-} embryos. (I–L') Whole-mount ISH and confocal images of *prox1* ISH and anti-GFP antibody staining in Control and *MZyap1*^{-/-} embryos. Figure 5—figure supplement 1. continued on next page

Figure 5—figure supplement 1. Continued

neuromasts (**D**), cell counts (**E**), and number of hair cells (**H**) per neuromast in the indicated experimental conditions. Cell counts were performed in the neuromast closest to the end of yolk extension (n3 or n4) at 72 hpf in (**E–H**). (**F–G'**) MIP of Z-stacks of a deposited neuromast (n3 or n4) stained with an anti-HCS1 antibody (hair cells, red) and DAPI (cell nuclei, blue). (**I–L'**) ISH with a *prox1* probe and an anti-GFP antibody staining (**J', L'**) on embryos with the indicated genetic background. Red arrows point to the pLLP (**A, B, I** and **K**) (**Figure 5—source data 3, 4**).

DOI: [10.7554/eLife.08201.029](https://doi.org/10.7554/eLife.08201.029)

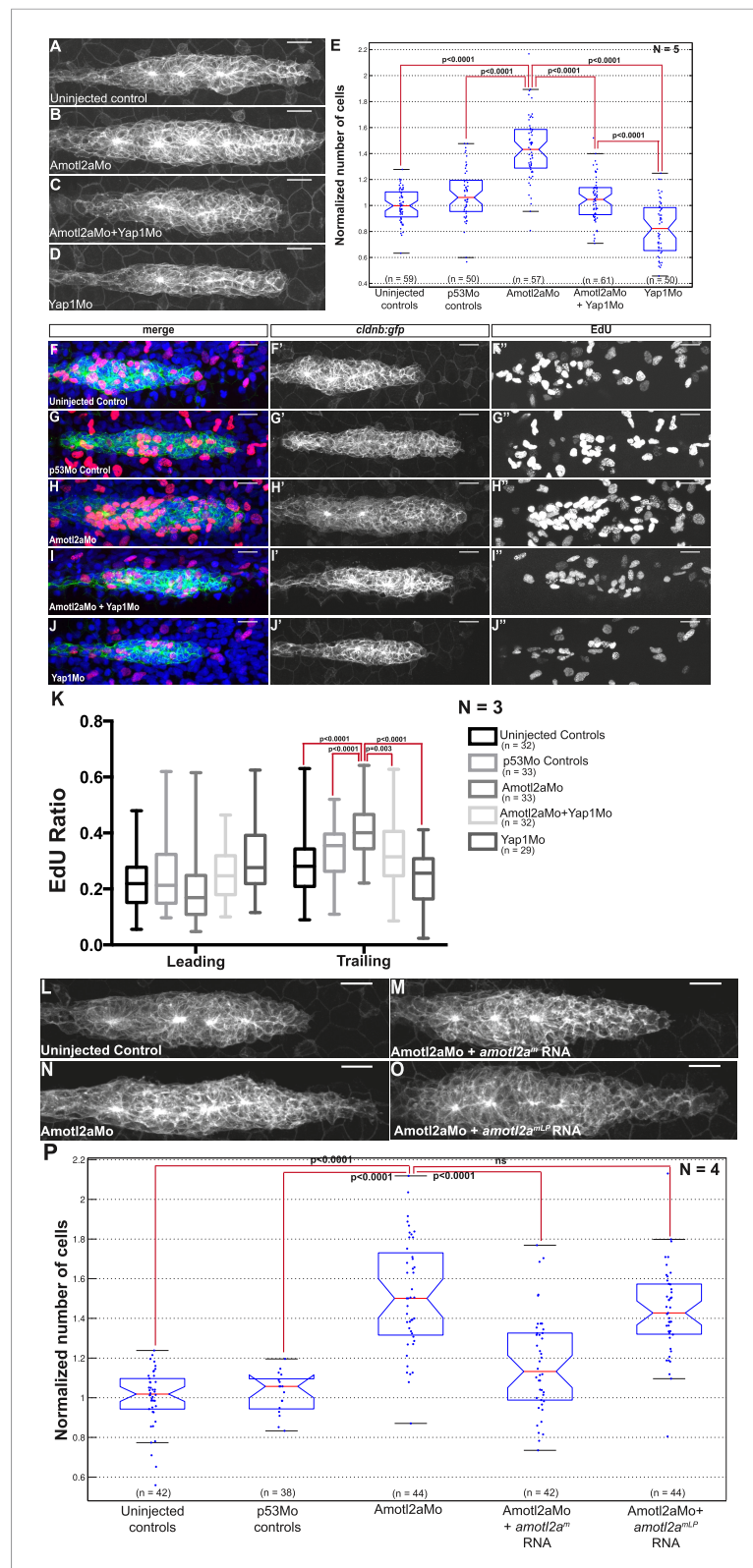


Figure 6. Loss of Yap1 suppresses the increased cell proliferation in *amotl2a* morphant. (A–D, L–O) MIP of Z-stacks of pLLP in *cldnb:gfp* embryos injected as indicated. (E, P) Corresponding boxplots comparing pLLP cell counts. (F–J') MIP of Z-stacks of pLLP in *cldnb:gfp* embryos stained with EdU and DAPI showing the EdU (right panels), cell membranes (middle panels), and merged channels (left panels). (K) Corresponding boxplot showing the EdU index.

Figure 6. Continued

in the leading and trailing regions of the pLLP in the indicated experimental conditions (**Figure 6—source data 1–3; Figure 6—figure supplement 1, Figure 6—source data 4**).

DOI: [10.7554/eLife.08201.030](https://doi.org/10.7554/eLife.08201.030)

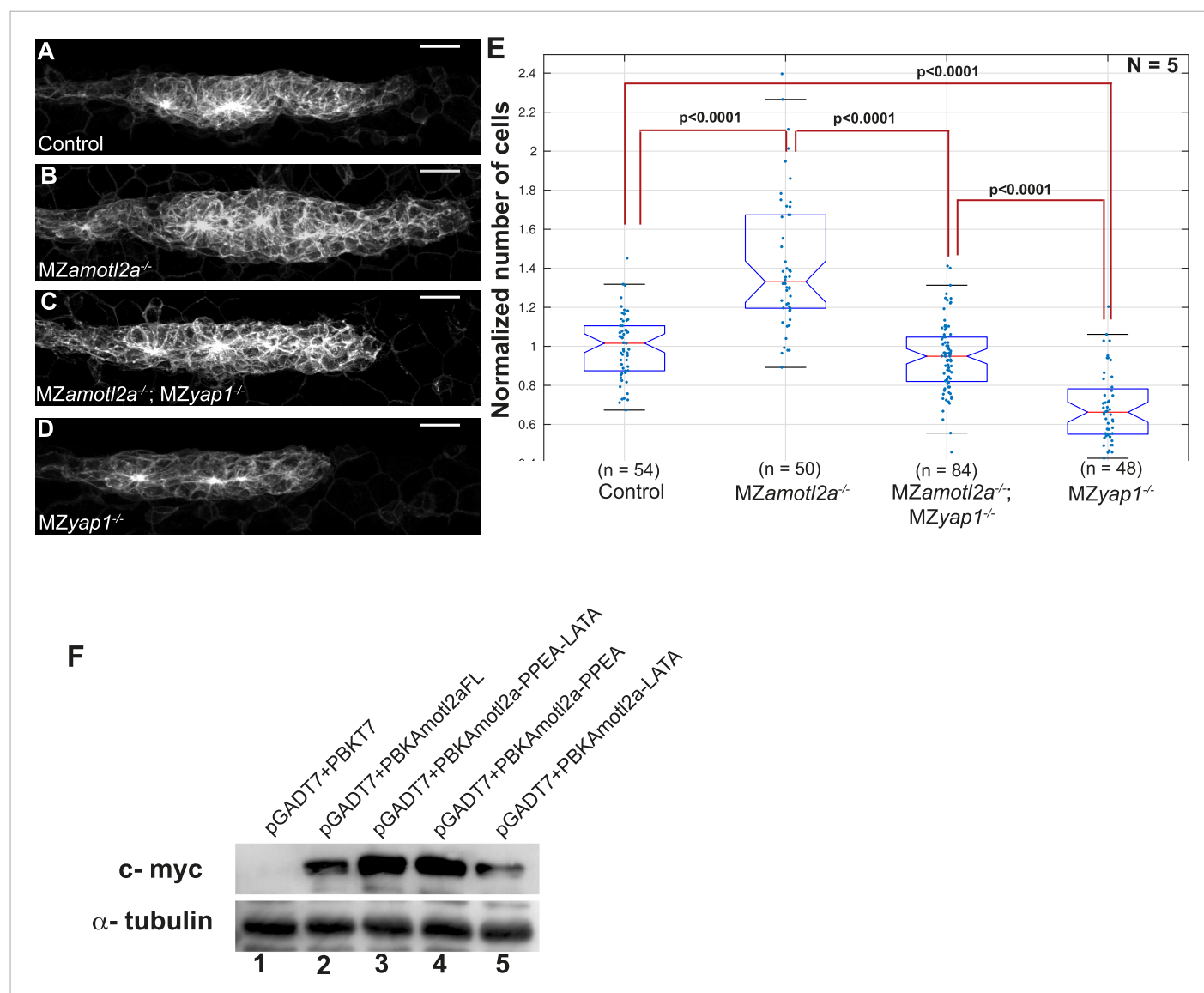


Figure 6—figure supplement 1. Loss of Yap1 in *MZamotl2a^{-/-}; MZyap1^{-/-}* embryos suppresses increased pLLP cell number resulting from loss of Amotl2a in *MZamotl2a^{-/-}* embryos. The mutation of Yap1-binding domains in Amotl2a does not render it unstable. MIP of Z-stacks of pLLP in *cldnb:gfp* embryos with the indicated genotype (A–D). (E) Corresponding boxplot comparing pLLP cell counts. (F) Western blot showing the stability of wild-type Amotl2a, Amotl2aFL (lane2) and Amotl2a forms carrying both PPEA-LATA (lane3) and single PPEA and LATA (lanes 4 and 5), respectively. α-tubulin staining shows equal protein loading (Figure 6—source data 4).

DOI: [10.7554/eLife.08201.035](https://doi.org/10.7554/eLife.08201.035)

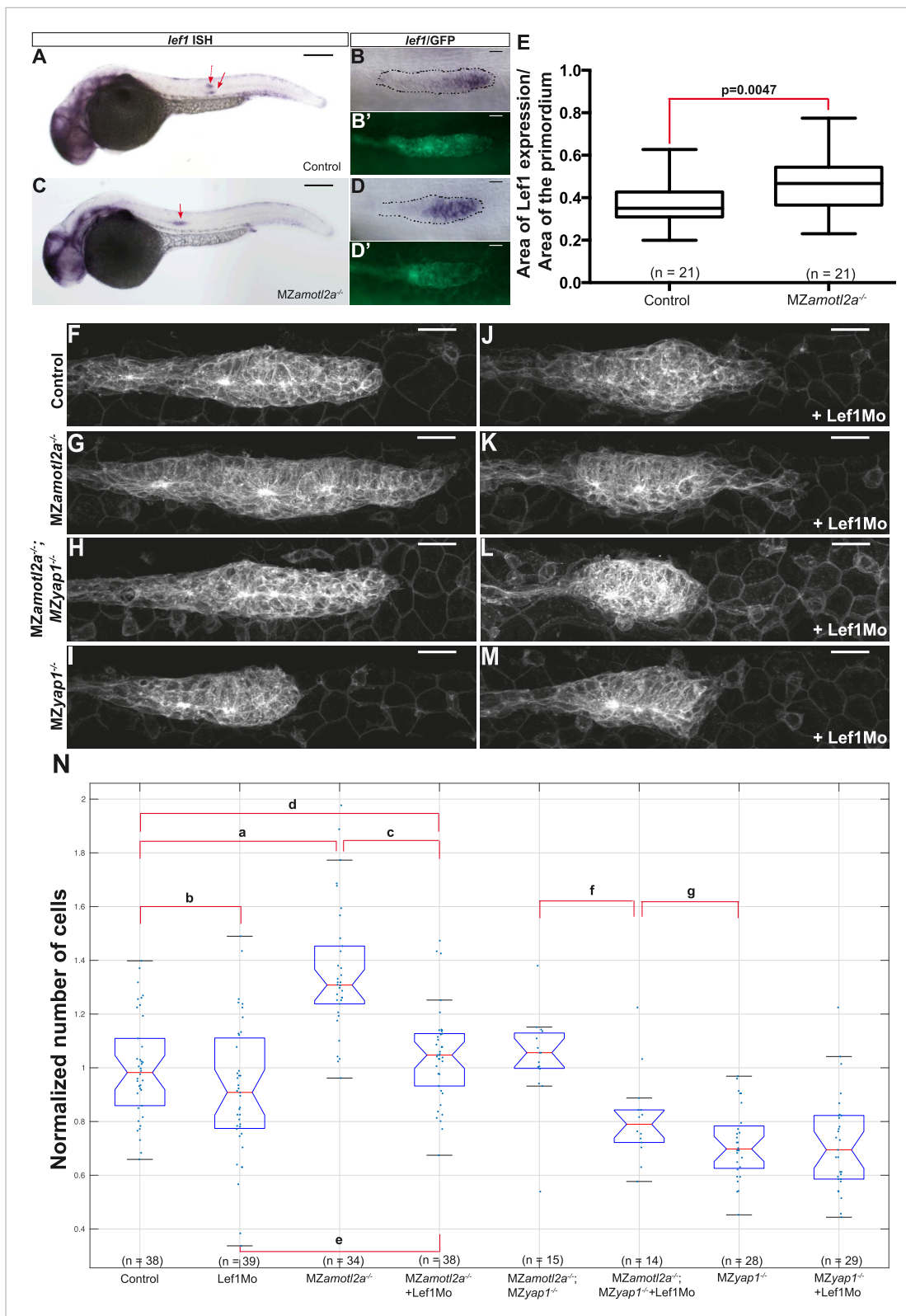


Figure 7. Loss of *Lef1* suppresses the increased cell proliferation in *amotl2a* mutants. (**A-D'**) 30 hpf *clnbn:gfp* embryos with the indicated genetic background stained with a *lef1* ISH probe and an anti-GFP antibody (**B'**, **D'**). (**E**) Boxplot showing the expansion of *lef1* expression domain in *MZamotl2a^{-/-}* embryos. (**F-M**) MIP of Z-stacks of pLLP in *clnbn:gfp* embryos with the indicated genotype, either uninjected (**F-I**) or injected with a *Lef1*Mo (**J-M**). (**N**) Corresponding boxplot comparing pLLP cell counts (**Figure 7—source data 1, 2; Figure 7—figure supplement 1, Figure 7—source data 3**). DOI: 10.7554/eLife.08201.036

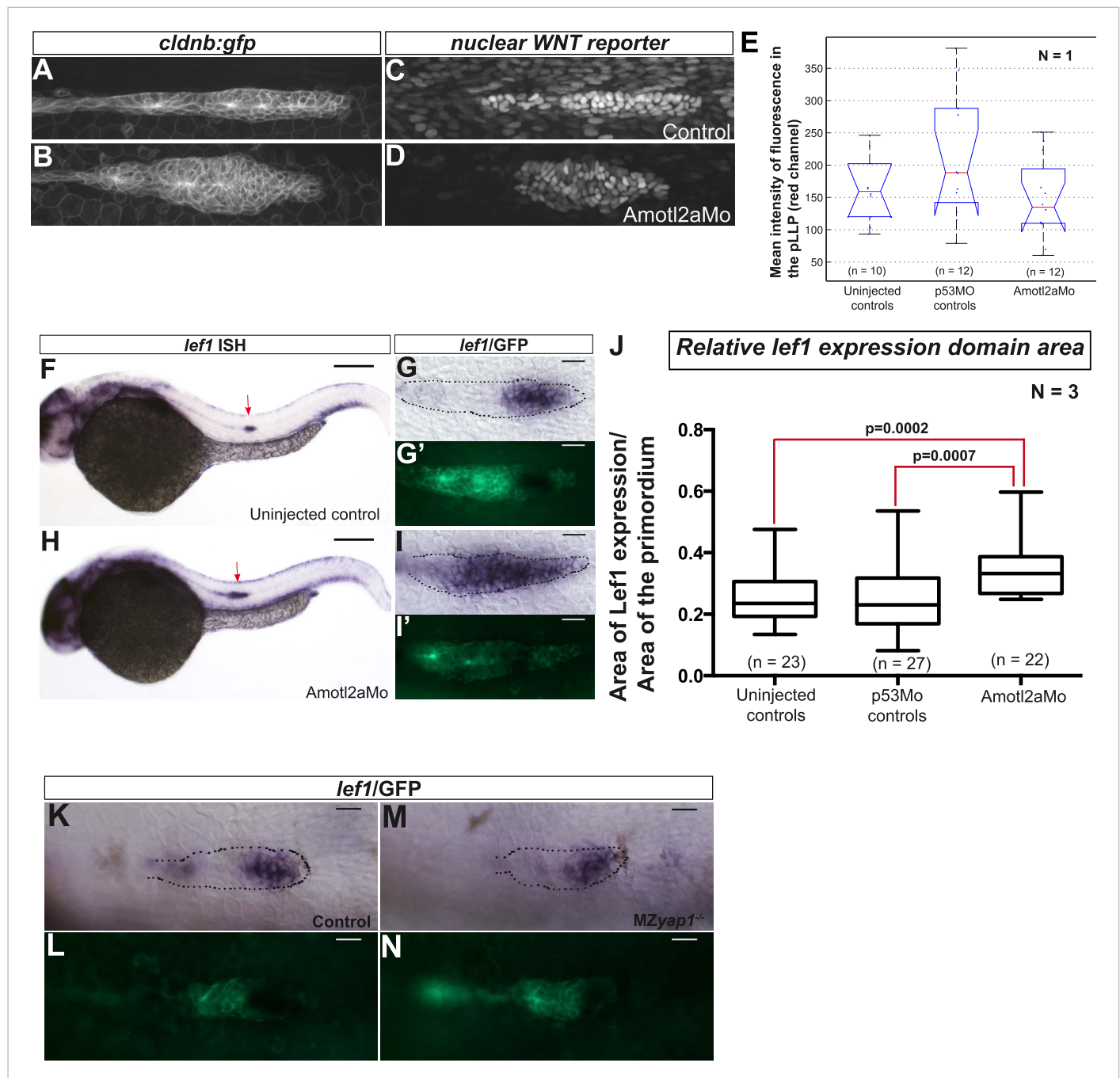


Figure 7—figure supplement 1. Loss of *Amotl2a* leads to an expansion of *lef1* expression. (A–D) MIP of confocal stacks of the pLLP in *Tg(7xTCF-Xla.Sia:NLS-mCherry)* embryos injected (B, D) or not injected (A, C) with the *amotl2a*Mo and showing the green (membranes, left) and red (nuclear WNT reporter) channels. (E) Boxplot comparing the relative mean intensity of fluorescence in the red channel in the corresponding pLLP. (F–I') Overview pictures (F, H) and close-up on the pLLP of 30 hpf *cldb:gfp* embryos injected (H, I, I') or not injected (F, G, G') with the *Amotl2a*Mo and stained with a *lef1* ISH probe and an anti-GFP antibody (G', I'). Red arrows point to the pLLP (F, H). (J) Boxplot showing the expansion of *lef1* expression domain in *amotl2a* morphants. (K–N) Close-up on the pLLP of 30 hpf control or *MZyap1*^{-/-} *cldb:gfp* embryos stained with a *lef1* ISH probe and an anti-GFP antibody (L, N). The relative *lef1* expression domain is not different in *MZyap1*^{-/-} embryos (Figure 7—source data 3).

DOI: 10.7554/eLife.08201.040

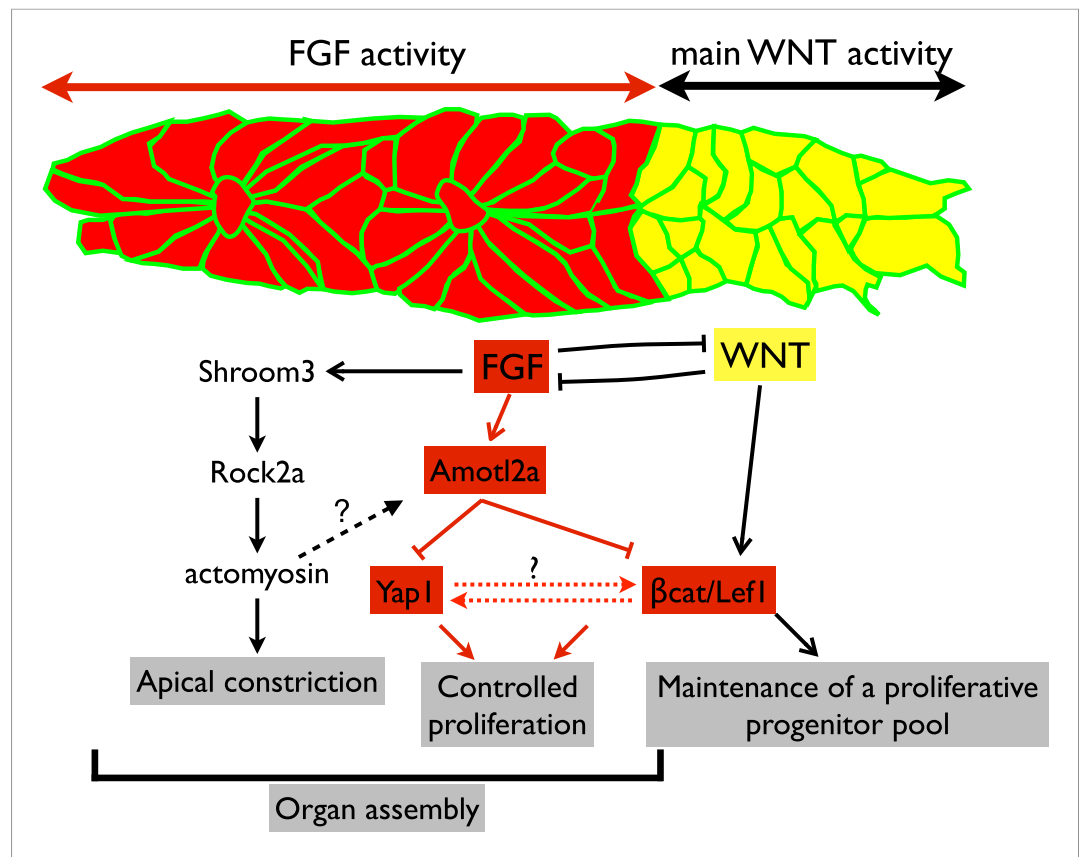


Figure 8. Working model. Scheme summarizing the main regulatory pathways involved in proliferation control and organ formation in the pLLP. The red part corresponds to new findings from the present study. Dotted lines indicate hypothetical links.

DOI: [10.7554/eLife.08201.041](https://doi.org/10.7554/eLife.08201.041)